IMPACT OF NON-IDEAL ANTENNAS ON THE PERFORMANCE OF UWB IMAGING SYSTEMS

Malgorzata Porebska[*], Jens Timmermann[*], Christian Sturm[*], Thomas Zwick[*], and Werner Wiesbeck[*]

Abstract: In this paper the influence of non-ideal antennas on the quality of UWB imagery is analyzed. The frequency dependent patterns of different antennas are measured and inserted into a simulation model. The obtained raw data are focused using the Kirchhoff migration method and the positions of the simulated scatterers are extracted. Using these data the positioning error, resolution, and coverage of an imaging system are analyzed in connection to the antenna features.

Introduction

Since the approval of ultra-wideband (UWB) spectrum by the Federal Communications Commission (FCC) in 2002 the UWB systems are gaining more and more attention of researchers and of industry. While high-rate communication systems seem to be the main application of UWB also localization and radar systems can profit from the extremely large bandwidth. In recent years a number of approaches for UWB imaging and target identification have been successfully tested for ultra-wideband [1, 2].

The purpose of this paper is to investigate the influence of the antenna pattern and its wideband properties on the imaging capabilities, assessing the dependence of the positioning error, the resolution and the coverage on the antenna features. The remainder of this paper is organized as follows: First, a short description of the used imaging approach is given followed by an introduction of the considered UWB antennas. Finally, the simulation method and results are described and conclusions are given.

Imaging approach

The imaging method under consideration is Kirchhoff migration [1, 2]. The sensor consisting of the transmitter and receiver antenna is moved along a linear route. Each scatterer in the illuminated area results with a hyperbolical wave front in the received signal. The image is calculated as follows: first a grid $O(x,y)$ is generated for the area of interest. For each point of the grid a point scatterer is assumed, and the distance between this scatterer and the sensor is calculated, then the values of the measured data are found for this distance. Repeating this procedure for all antenna positions delivers the final image. This is expressed by the following equation:

$$O(x,y) = \sum_{n=1}^{N} h_n\left(t - \frac{r_{Tx_n} + r_{Rx_n}}{c}\right)$$

where $h_n(t)$ is the impulse response measured at the n-th sensor position, r_{Tx_n} is the distance between the transmitter and the considered scatterer, r_{Rx_n} is the distance between the scatterer and the receiver, and c indicates the velocity of light. A single scatterer appears in each single step as an arch consisting of points with the same distance to the sensor. Through the summation over multiple sensor positions different arches are superimposed giving a high value at the real position of scatterer.

Antennas for UWB

Four different antennas are considered: two directive antennas including a commercially available broadband quad ridged horn antenna (EM Systems, A6100) and a Vivaldi antenna [3], and two omnidirectional ones including an aperture coupled bow-tie antenna [4] and as a reference a fictive, ideal omnidirectional antenna. The parameters of these antennas for the considered frequency band of 3 – 10 GHz are summarized in table 1. All antennas except for the omnidirectional reference are measured in an anechoic chamber. The resulting gain over frequency is depicted in Fig. 1.

---

[*] Institut für Höchstfrequenztechnik und Elektronik, Universität Karlsruhe (TH)
Kaiserstr 12, 76131 Karlsruhe, Germany
malgorzata.porebska@ihe.uka.de

Antenna	Gain in dBi	Beamwidth in deg.
Horn	7.7 (3GHz) - 15.2 (10 GHz)	70 (3 GHz) - 24 (10 GHz)
Vivaldi	3.3 (3 GHz) - 8 (10 GHz)	100 (3 GHz) - 40 (10 GHz)
Bow-tie	0 (3 GHz) - 6 (3 GHz)	360

Tab. 1 Features of the used antennas

(a) Quad ridged horn antenna

(b) Vivaldi antenna
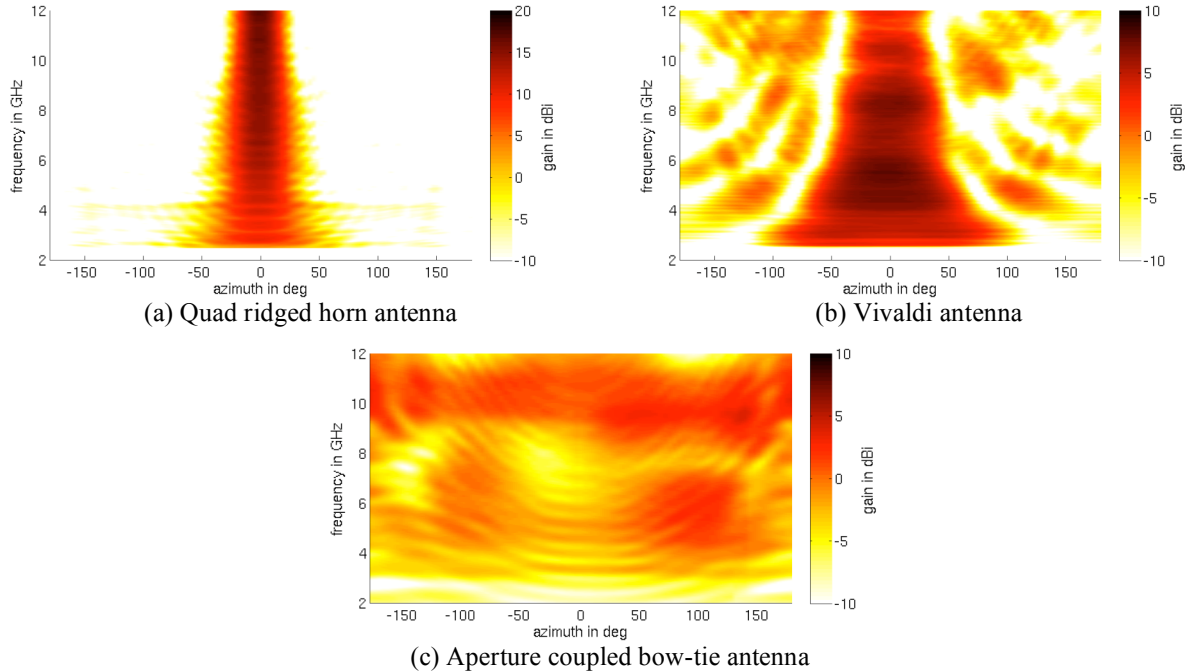
(c) Aperture coupled bow-tie antenna

Fig. 1 Antenna gain measured over the frequency

It is expected that the wideband characteristics of the antennas [3] have a considerable influence on the quality of the obtained image: UWB antennas show frequency- and angle-dependent behavior. In time domain this leads to additional direction dependent delay imposed by the antennas on the received signal. As the considered imaging approach utilizes information about the propagation time, this additional delay can lead to uncertainties in the obtained image.

Simulation results

The simulation scenario contains a sensor (Tx and Rx) moving on a linear track along the *x*-axis, scanning the half plane in front of the antennas. The transmitter antenna is placed 20 cm above the receiver antenna. The length of the track is 4 m and the distance between the single sensor positions is 5 cm.

First, the influence of the antenna on the positioning error is investigated. A single, perfectly electrical conducting object is placed in the free space in front of the sensor under different angles in respect to the midpoint of the sensor track. The 0 degree direction is equivalent to the normal of the considered track. Two distances of 1 m and 5 m between the scatterer and the middle of the track are considered. For each angle the position of the object is determined from the migrated image and compared to the original position of the target. From the deviation in *x*- and *y*-directions the root mean square error is calculated. In Fig. 2 the positioning error dependent on the investigated antenna is shown. Additionally, in Tab. 2 the averaged error values for angles from 0 to 85° are given.

Antenna	d = 1 m	d = 5 m
Omni	$1.1 \cdot 10^{-3}$	$4.2 \cdot 10^{-3}$
Horn	$4.9 \cdot 10^{-3}$	0.109
Vivaldi	$2.5 \cdot 10^{-3}$	$5.4 \cdot 10^{-3}$
Bow-tie	$1.8 \cdot 10^{-3}$	$2.7 \cdot 10^{-3}$

Tab. 2 Mean positioning error in m
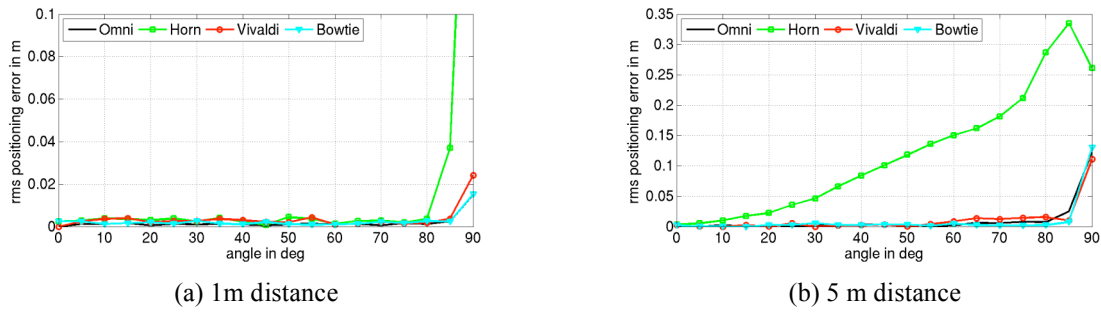
| (a) 1m distance | (b) 5 m distance |

Fig. 2 Positioning error vs. scatterer position

The position of the scatterer can be reconstructed from the migrated image with a great precision in almost all cases. At the angle of 90° the image of the scatterer is wider and its position is harder to identify. Thus the error for this direction is greater than for the remaining positions. The scatterer in 1 m distance track stays in the range of the sensor track all the time, thus even at higher angles the target can be seen in front of the antenna for at least few sensor positions. In the 5 m case the target stays in front of the sensor track only for angles up to 23.6°. This results with high error values for the horn antenna. On the other hand the error values for the Vivaldi antenna stay low. This suggests that the positioning error is rather dependent on the angle-dependent transfer function of the antenna than on the radiation pattern itself.

For the resolution estimation a set of colinear point scatterers is placed in front of the sensor. Both range and cross-range directions are considered. In the cross-range case the point scatterers are placed along the x-axis in the distance of 2 m to the sensor track (cf. Fig. 3(a)) whereas in the range case the targets are placed along the y-axis and the first target is placed 1 m away from the midpoint of the sensor track. The distance d between single scatterers is varied between 5 mm and 20 cm. We assume that two targets are distinguishable when both targets cause local maxima separated by a local minimum, the value of which is at most 70% of the maximum value in the image. The distances, at which the single scattering points are distinguishable for the considered antennas are given in table 3. The obtained resolution in cross-range is influenced strongly by the shape of the single target image and is thus dependent on the pattern of the antenna. For directive antennas this image is wider and the distance between the targets have to be larger in order to distinguish them, whereas in the case of omnidirectional antennas the image of the target is very compact and allows for better resolution. The range resolution is very similar for all considered antennas and seems to be independent of the pattern. The achieved resolution in range and cross-range is approximately equal to the size of the image of a single target for each antenna.
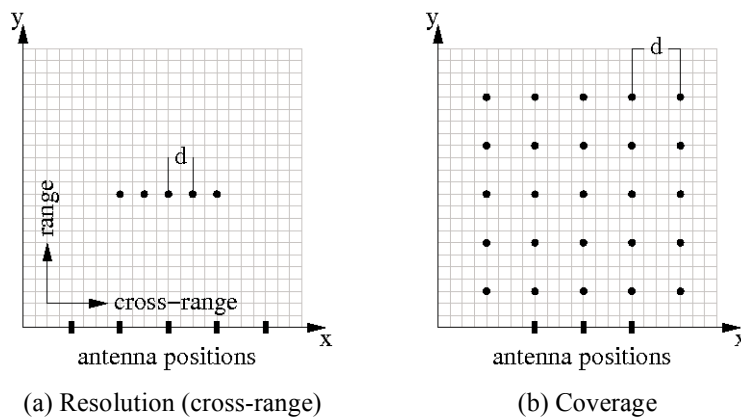

| (a) Resolution (cross-range) | (b) Coverage |

Fig. 3 Test scenarios

In the last step the coverage is examined using point scatterers placed on a grid with a spacing of 1 m. In the x-direction the scatterers are placed also outside of the sensor track (cf. Fig. 3(b)). The coverage in range is not only dependent on antenna properties but also on the placement of the scatterers. The scatterers in the proximity of the sensor generate artifacts, which may be stronger than the contributions from distant scatterers. In this case the distant targets cannot be distinguished from the artifacts. Thus the coverage of the imaging system is much smaller in the presence of near targets. If only distant scatterers are considered, the coverage is only limited by the sensitivity of the receive system. Fig. 4 depicts the obtained image of a grid of scatterers for an omnidirectional and for the horn antenna. The point (0,0) corresponds to the midpoint of the sensor track, which is placed on the x-axis. The visible points correspond to the targets and the coverage is defined by the position of the targets that are visible in the image. In table 3 the values of the coverage in the presence of near targets are

summarized. There is a strong correspondence to the pattern of the antenna: The omnidirectional antennas are able to localize also the targets that are far from the track in cross-range, whereas the cross-range coverage of directive antennas is limited to positions in front of the sensor track. On the other hand the directive antennas are able to detect objects, which are placed far away from the sensor track if they are placed in the main beam of the antenna.

Antenna	Resolution		Coverage	
	range	cross-range	range	cross-range
Omni	11 mm	20 mm	12 m	24 m
Horn	9 mm	90 mm	24 m	4 m
Vivaldi	11 mm	28 mm	18 m	6 m
Bow-tie	12 mm	20 mm	14 m	20 m

Tab. 3 Resolution and coverage for different antennas
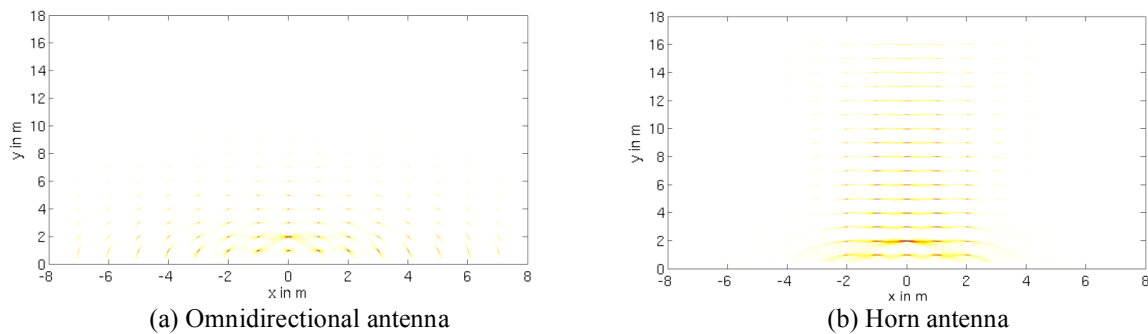

(a) Omnidirectional antenna

(b) Horn antenna

Fig. 4 Coverage of migration algorithm

Conclusions

In this paper the influence of the antenna features on UWB imagery is described. The Kirchhoff migration scheme is applied to the simulation, in which different real UWB antennas and a theoretical ideal omnidirectional antenna are embedded. Using the migrated images the influence of the antenna pattern on positioning error, resolution and coverage of an ideal imaging system is analyzed. It is shown that the positioning error is dependent rather on the angle-dependent transfer function of the antenna than on the radiation pattern. The cross-range resolution is influenced by the antenna pattern as the image of a single scatterer obtained by using a directive antenna is wider and thus the distance between two distinguishable points has to be larger. On the other hand the range resolution does not show any dependence on the antenna features. Also the coverage is shown to be dependent on the antenna radiation pattern with omnidirectional antennas having larger coverage in the cross-range and directive antennas having larger coverage in range.

Acknowledgment

References

[1] R. Zetik, J. Sachs, and R. Thomä, "Imaging of propagation environment by UWB channel sounding," in *XXVIIIth General Assembly of URSI, New Delhi, India*, Oct. 2005.

[2] S. Hantscher, B. Praher, A. Reisenzahn, and C. Diskus, "Comparison of UWB target identification algorithms for through-wall imaging applications," in *3rd European Radar Conference, EuRAD 2006*, Sept. 2006, pp. 104–107.

[3] W. Sörgel and W. Wiesbeck, "Influence of the antennas on the ultra wideband transmission," *EURASIP Journal on Applied Signal Processing, special issue UWB - State of the Art*, pp. 296–305, Mar. 2005.

[4] W. Sörgel, C. Waldschmidt, and W. Wiesbeck, "An ultra wideband aperture coupled bow tie antenna for communications," in European Electromagnetics Symposium, 2004.